

Optimal Radio Resource Allocation for Hybrid Traffic in Cellular Networks: Centralized and Distributed Architecture

Mo Ghorbanzadeh, Ahmed Abdelhadi, and Charles Clancy

Abstract—Optimal resource allocation is of paramount importance in utilizing the scarce radio spectrum efficiently and provisioning quality of service for miscellaneous user applications, generating hybrid data traffic streams in present-day wireless communications systems. A dynamism of the hybrid traffic stemmed from concurrently running mobile applications with temporally varying usage percentages in addition to subscriber priorities impelled from network providers' perspective necessitate resource allocation schemes assigning the spectrum to the applications accordingly and optimally. This manuscript concocts novel centralized and distributed radio resource allocation optimization problems for hybrid traffic-conveying cellular networks communicating users with simultaneously running multiple delay-tolerant and real-time applications modelled as logarithmic and sigmoidal utility functions, volatile application percent usages, and diverse subscriptions. Casting under a utility proportional fairness entail no lost calls for the proposed modi operandi, for which we substantiate the convexity, devise computationally efficient algorithms catering optimal rates to the applications, and prove a mutual mathematical equivalence. Ultimately, the algorithms performance is evaluated via simulations and discussing germane numerical results.

Index Terms—Utility function, Hybrid traffic, Convex optimization, Centralized algorithm, Distributed algorithm, Optimal resource allocation, Dual problem.

I. INTRODUCTION

Mobile broadband services have been falling afoul of a perennially upsurged demand for radio resources during recent years. This upswing owes to the gigantic boom in mobile service subscribers' quantity as well as to the outgrowth of their generated traffic volume [2]. On the other hand, the migration of cellular network providers from offering a single service such as the Internet access to a multi-service framework, like multimedia telephony and mobile-TV [3], along with the emergence and prevalence of smartphones hosting simultaneously running delay-tolerant and real-time applications with distinctive quality of service (QoS) requirements [4] arise an urgency to dynamically provisioning various bit rates to the application traffic so as to elevate users' quality of experience (QoE) tightly bound to the subscriber churn [3]. As such, incorporating service differentiation mechanisms into resource allocation methods is a matter of high consequence. Inasmuch as applications' temporal usage percentage directly impacts the generated traffic volume and nature, e.g. the

traffic elasticity, including the usage percentage as an application status differentiation in resource allocation schemes is worthwhile. Besides, cellular network providers capability to adopt a subscription-based differentiation [3], wherein miscellaneous clients of an identical service receive differentiated subscription-based treatments (corporate vs. private, post-paid vs. pre-paid, and privileged vs. roaming users), can fine-tune resource allocation approaches. Henceforth, resource allocation modi operandi can accommodate diverse exigencies of present-day wireless networks conveying the hybrid traffic by accounting for all the aforementioned issues. Nonetheless, the majority of resource allocation proposals fizzle to address the aforesaid concerns collectively (section I-A).

This paper puts forward a novel convex utility proportional fairness maximization formulation for an optimal resource allocation in wireless networks and is outfitted with the subscriber, application status, and service differentiations parameterized respectively as user equipment (UE) subscription weights, application status weights, and application utility functions. The weights are supplied by network providers so that a foreground-running application such as a voice call attains a higher application status weight than do the background-running ones, e.g. an automatic application update process. Mobile subscribers of the system under our consideration can concurrently run multiple applications with their utility functions and statuses depending on the generated traffic nature and instantaneous usage percentage, respectively.

Moreover, casting the service differentiation under a utility proportional fairness policy prioritizes the real-time traffic over the delay-tolerant one, conducive to fulfilling QoS requirements. In addition to solving the formalized optimization problem analytically, we develop distributed and centralized solution procedures as computationally efficient algorithms excerpted from Lagrangians of the resource allocation's dual problems [5] and perform necessary simulations to validate leveraged methodologies. For the distributed case, the rate assignment process is realized in double stages which first optimally allocates UEs the Evolved Node B (eNB) resources via their mutual collaborations and then disseminate UE bandwidths to the running applications internally to the UEs in an optimum fashion. In contrast, the devised centralized routine allots hybrid application rates in a monolithic stage transacted in the cellular network provider side of the communications system.

Part of this work was accepted at IEEE ICNC CNC Workshop 2015 [1].

M. Ghorbanzadeh, A. Abdelhadi, and C. Clancy are with the Hume Center for National Security and Technology, Virginia Tech, Arlington, VA, 22203 USA e-mail: {mgh, aabdelhadi, tcc}@vt.edu.

A. Related Work

The resource allocation optimization research area has received a significant attention since the seminal network utility maximization study in [6] which allocated user rates through a utility proportional fairness maximization solved by the Lagrange multipliers [5]. Soon after, an iterative algorithm relying on the duality of the aforementioned resource allocation problem was proposed [7]. Whilst the traffic in these early research works had an elastic nature common for wired communication systems and approximated by concave utility functions, the advent and prevalence of high-speed wireless networks have entailed an increased utilization of real-time applications whose utility functions grow non-concave [8]. For instance, the utility of a voice-over-IP (VoIP) can be represented as a step function whose utility is zero before a certain threshold rate and achieves 100% for rates larger than the threshold. Another example is a video streaming application whose utility can be approximated as a sigmoidal function convex (concave) for rates below (above) its inflection point. As such, the methods presented in ([6], [7]) incur the proceeding drawbacks: (a) Reaching optimal solutions for solely concave utility functions, they are inapplicable to the drastically escalating inelastic traffic volume of our networks; (b) Neither priority do they render to real-time applications with stringent QoS requirements, nor they reserve any attention for the application statuses, nor they look after subscribers' varied importance pivotal from a business standpoint.

Later, the authors in ([9], [10]) presented distributed rate allocation algorithms for multi-class service offerings based on concave and sigmoidal utility functions representing applications. Despite closely approximating optimal solution, involved methods dropped users to maximize the system utility, so they could not guarantee a minimal QoS. An effort by the authors in ([11]–[13]) proposed a utility proportional fairness resource allocation, for users of a single-carrier communication network, cast as a convex problem with logarithmic and sigmoidal utility functions respectively modelling delay-tolerant and real-time applications. Although their schemes prioritized the real-time applications over the delay-tolerant ones, they neither contemplated the application status or user differentiation concepts, nor regarded the hybrid traffic prevailing in modern networks.

In [14], the author considered a weighted aggregation of logarithmic and sigmoidal utilities approximated to the nearest concave utility function via a minimum mean-squared error measure inside UEs. The approximate utility function solved the rate allocation optimization through a variation of the conventional distributed resource allocation approach in [6] such that rate assignments essentially estimated optimal ones. However, the rate were only approximations and no consideration was given to user or application priorities. This work was extended by Shajaiah et. al. ([15], [16]) to allow for the application of the resource allocation in a multi-carrier network in public safety. The authors in ([17], [18]) considered a similar multicarrier optimal resource allocation aware of the subscriber priorities. However, no attention was

rendered to the temporal changes in the application usage or UE quantities. In ([19]), the authors adopted a non-convex optimization formulation to maximize the system utility in wireless networks consisting of applications with logarithmic and sigmoidal utility functions. A distributed process was employed to obtain the rates under a zero duality gap; but, the algorithm did not converge for a positive duality gap leading to compounding a heuristic to ensure the network stability.

In other studies, the authors of [20] created a utility max-min fairness resource allocation for the hybrid traffic sharing a single path in a communications network. Similarly, [21] presented a utility proportional fairness optimization for the high signal-to-interference-plus-noise ratio wireless networks using a utility max-min architecture, contrasted against the traditional proportional fairness algorithms [22] and provided a closed-form solution that refrained from network oscillations. However, neither methods cared for any traffic or user priorities in assigning the spectrum. In ([23], [24]), the authors developed a utility proportional fairness resource block allocation in wireless networks as an integer optimization problem. They initially obtained the continuous optimal rates and then took on a boundary mapping technique to extracted a pool of valid resource blocks tantamount to inferred optimal continuous rates, albeit neither hybrid traffic, nor application status, nor user importance was taken into the equation. In a similar work [25], the authors organized a utility proportional fairness optimization which allocated optimal UE rates in a cellular infrastructure coexistent with radars by leveraging the Lagrange multipliers. Finally, [26] presented a subcarrier allocation in orthogonal frequency division multiplexed systems concentrating on delay constrained data and used network delay models [27] for the subcarrier assignment. And last but not the least, [28] developed a location/time/context-aware source allocation in cellular networks; however, they did not consider the temporal changes in the application usage percentage, the number of UEs, or subscribers' priority.

B. Contributions

In brevity, contributions of the current manuscript proceed as such.

- We formulate resource allocation optimizations with centralized and distributed architectures for cellular communication systems subsuming smartphones generating a hybrid traffic of elastic and inelastic data flows respectively stemmed from concurrently running delay-tolerant and real-time applications applications mathematically modelled as logarithmic and sigmoidal utility functions in that order.
- We prove that the proposed resource allocation optimization problems are convex, have tractable global optimal solutions (the rate assignments are optimal), render bandwidth assignment priorities to real-time applications due to their reliance on the utility proportional fairness framework, and eschew from dropping users hereby a minimum QoS is warranted.
- We adopt a two-stage algorithm for the distributed approach to optimally assign rates for UEs externally and for running applications internally.

- We derive a robust one-stage algorithm for the centralized scheme to optimally assign rates to the running applications externally to the UEs and prove that the mathematical equivalence of the two-stage and one-stage concocts.

C. Organization

The remainder of this paper is organized as follows. Section I-A surveys the topical resource allocation literature in brevity. Section II presents the formulation for the centralized and distributed resource allocation optimizations problems. Section III proves the existence of global optimal solutions for the optimization problems devised in section II. Section IV puts forward solution algorithms for the optimization problems. Section VI proves the mathematical equivalence between the distributed and centralized algorithms. Section IV-C illustrates the distributed robust rate allocation algorithm to refrain from rate fluctuations. Section V provides with a solution algorithm for the one-stage centralized rate allocation algorithm. Section VII discusses simulation setup and develops quantitative results along with their analysis for the implementation of the proposed resource assignment schemes. And, section VIII concludes the paper.

II. PROBLEM FORMULATION

The objective is to determine optimal rates that hybrid-traffic-carrying cellular communications systems should be allocating to their UE applications so as to dynamically ensure as such: 1) Real-time applications are rendered priority over delay-tolerant ones. 2) no user is dropped 3) Applications temporal usage is accounted for. 4) Subscription-based treatments is honored. We assume each UE contains multiple simultaneously running real-time and delay-tolerant applications, mathematically represented by sigmoidal and logarithmic utility functions as shown in section II-A.

A. Applications Utility functions

Utility function have been used in a wide variety of research works to model some representative characteristic of the system. For instance, [29] leveraged utility functions to model the modulation schemes in a power allocation problem. In this paper, an application performance satisfaction as a function of its allocated rates is referred to as a utility function, denoted as $U(r)$ for the rate r , and have the following properties [8].

- $U(0) = 0$ and $U(r)$ is an increasing function r .
- $U(r)$ is twice differentiable in r and bounded above.

The first statement of the former property implies the nonnegativity of the utility functions which is expected since they represent application performance satisfaction percentage, whereas its second statement reveals that the more assigned rate, the higher the application performance satisfaction. On the flip side, the latter property indicates the continuity of the utility functions. Hybrid traffic consists of elastic and inelastic traffic streams sprung from respectively delay-tolerant and real-time applications whose utilities are conductively

modelled by correspondingly normalized logarithmic and sigmoidal utility functions in equations (1) and (2) in that order ([10]).

$$U(r) = c \left(\frac{1}{1 + e^{-a(r-b)}} - d \right) \quad (1)$$

Here, $c = \frac{1+e^{ab}}{e^{ab}}$ and $d = \frac{1}{1+e^{ab}}$. It can be easily verified that $U(0) = 0$ and $U(\infty) = 1$, where the former is one of the previously mentioned utility function properties and the latter indicates that an infinite resource assignment ensues 100% satisfaction. Furthermore, it is easily derivable that the inflection point of equation (1) occurs at $r = r^{\text{inf}} = b$, where the superscript "inf" stands for inflection.

$$U(r) = \frac{\log(1 + kr)}{\log(1 + kr^{\text{max}})} \quad (2)$$

Here, r^{max} is the maximum rate at which the application QoS is satisfied in full (100% utility percentage) and k is the utility function increase with augmenting the allocated rate r . It can be easily checked that $U(0) = 0$ and $U(r^{\text{max}}) = 1$, where the former is again the basic property of the utility functions and the latter implies that a 100% QoS satisfaction occurs at $r = r^{\text{max}}$. Moreover, the inflection point of normalized logarithmic function is at $r = r^{\text{inf}} = 0$. For the sake of illustration, the utility functions with the parameters according to Table I are plotted in Figure 3(a), from which we can observe that the sigmoid utility functions gain a slight QoS satisfaction only after the allocated rates surpass the inflection points of the utilities whereas the logarithmic ones obtain some QoS fulfillment even for a minuscule assigned bandwidth. These behaviors make sigmoidal and logarithmic utility functions suitable for modeling real-time and delay-tolerant applications respectively, and the germane mathematical analyses appear in ([10], [21]) in nuance.

Next, section II-B concocts the system model for the rate allocation problem proposed in this article.

B. System Model

To present the system, with no loss of generality, we concentrate on a cellular network's single cell, which subsumes an eNB covering M UEs (here $M = 6$) depicted in Figure 1, where each UE concurrently runs delay-tolerant and real-time applications represented respectively by the logarithmic and sigmoidal utility functions in section II-A. The rate assigned by the eNB to the i^{th} UE is denoted as r_i and the UE's aggregated utility function is shown as $V_i(r_i)$, which we relate it to the UE application utilities accordingly to the equation (3) below.

$$V_i(r_i) = \prod_{j=1}^{N_i} U_{ij}^{\alpha_{ij}}(r_{ij}) \quad (3)$$

Here, r_{ij} , $U_{ij}(r_{ij})$, and α_{ij} respectively represent the rate allocation, application utility function, and application usage percentage of the j^{th} application running on the i^{th} UE. Hence, we can write $\sum_{j=1}^{N_i} \alpha_{ij} = 1$ and $r_i = \sum_{j=1}^{N_i} r_{ij}$, where, for the i^{th} UE, N_i is the number of coevally running

applications and r_i presents the bandwidth allotment by the eNB. The former of the afore-written equations states the fact that the addition of the i^{th} UE's application usage percentages proves 100% usage percentage, and the latter one implies that the i^{th} UE rate is the augmentation of all its N_i applications resources assignments.

We resort to a centralized and a distributed approach, illustrated in sections II-C and II-D respectively, to disseminate resources to the applications of UEs with the aggregated utility as in equation (3).



Fig. 1. System Model: Single cell, within the cellular network, with an eNB covering $M = 6$ UEs each with simultaneously running delay-tolerant and relay-time applications represented by logarithmic and sigmoidal utility functions respectively.

C. Centralized Optimization

We develop a rate allocation optimization problem that assigns the application resources directly by the eNB in a singular stage. The basic germane formulation is illustrated in equation (4).

$$\begin{aligned} \max_{\mathbf{r}} \quad & \prod_{i=1}^M \left(\prod_{j=1}^{N_i} U_{ij}^{\alpha_{ij}}(r_{ij}) \right)^{\beta_i} \\ \text{subject to} \quad & \sum_{i=1}^M \sum_{j=1}^{N_i} r_{ij} \leq R, \\ & r_{ij} \geq 0, \quad i = 1, 2, \dots, M, \quad j = 1, 2, \dots, N_i \end{aligned} \quad (4)$$

Here, for M UEs covered by an eNB, $\mathbf{r} = [r_1, r_2, \dots, r_M]$ is the UE allocated rate vector, R is the maximum available resources at the eNB, and β_i is a subscription-dependent weight for the i^{th} UE. Section III-C proves the convexity and tractable optimal solvability of the aforementioned optimization problem, whose solution procedure is concocted as an algorithm in section V.

Next, section II-D introduces a distributed approach to the resource allocation problem.

D. Distributed Optimization

We subdivide the optimization problem (4) into two simpler optimizations solved separately. The first optimization concerns with the UE rate allocation by the eNB via collaborations between the eNB and pertinent UEs hereby the optimization is referred to as external UE resource allocation (EURA). On the contrary, the second optimization wells up from distributing the application rates by the host UEs, performed internally to the UEs and is named the internal UE rate allocation (IURA). The solutions for the EURA and IURA optimization is laid as algorithms presented in section IV. The EURA formulation is explained below.

1) *EURA Optimization Problem:* EURA optimization, solved collaboratively amongst UEs and their eNB, can be written as equation (5), where $V_i(r_i) = \prod_{j=1}^{N_i} U_{ij}^{\alpha_{ij}}(r_{ij})$ is the i^{th} UE aggregated utility function expressed in equation (4), $\mathbf{r} = [r_1, r_2, \dots, r_M]$ is the UE rate vector whose i^{th} component represents the rate assigned by the eNB to the i^{th} UE, and M is the number of UEs covered by the eNB. In section III-A, we prove the convexity and tractable optimal solvability of the optimization problem in equation (5) exists and present the algorithm to solve this problem in section III.

$$\begin{aligned} \max_{\mathbf{r}} \quad & \prod_{i=1}^M V_i^{\beta_i}(r_i) \\ \text{subject to} \quad & \sum_{i=1}^M r_i \leq R, \\ & r_i \geq 0, \quad i = 1, 2, \dots, M. \end{aligned} \quad (5)$$

2) *IURA Optimization Problem:* IURA optimization problem, solved internally in each UE, can be written as equation (6) for the i^{th} UE with $i \in \{1, 2, \dots, M\}$, where $\mathbf{r}_i = [r_{i1}, r_{i2}, \dots, r_{iN_i}]$ is the application rate allocation vector such that its j^{th} component indicates the bandwidth allotted by the i^{th} UE to its j^{th} application, r_i^{opt} is the i^{th} UE rate allocated by eNB via solving the EURA optimization in equation (5), and N_i is the number of applications of the i^{th} UE. Superscript "opt" indicates the optimality of the UE rates which will be proved in section III-A. Besides, section III-B proves that there exists a tractable global optimal solution to the IURA optimization problem in equation (6) and section IV-D provides the solving algorithm thereof.

$$\begin{aligned} \max_{\mathbf{r}_i} \quad & \prod_{j=1}^{N_i} U_{ij}^{\alpha_{ij}}(r_{ij}) \\ \text{subject to} \quad & \sum_{j=1}^{N_i} r_{ij} \leq r_i^{\text{opt}}, \\ & r_{ij} \geq 0, \quad j = 1, 2, \dots, N_i. \end{aligned} \quad (6)$$

Next, section III proves the convexity of the EURA and IURA optimization problems.

III. EXISTENCE OF A GLOBAL OPTIMAL SOLUTION

This section proves the existence of optimal solutions for the centralized and distributed resource allocations developed in sections II-D and section II-C, respectively.

A. EURA Global Optimal Solution

Strictly increasing nature of logarithms yields in an equivalent EURA objective function $\arg \max_{\mathbf{r}} \sum_{i=1}^M \beta_i \log(V_i(r_i))$, stemmed from equation (5), reformulated and referred to as respectively equation 7 and log-EURA problem, for which the lemma III.1 is conceivable.

$$\begin{aligned}
& \max_{\mathbf{r}} \quad \sum_{i=1}^M \beta_i \log(V_i(r_i)) \\
& \text{subject to} \quad \sum_{i=1}^M r_i \leq R, \\
& \quad r_i \geq 0, \quad i = 1, 2, \dots, M.
\end{aligned} \tag{7}$$

Lemma III.1. *The aggregated utility natural logarithm $\log(V_i(r_i))$ is strictly concave.*

Proof: From equation (3), we can write $\log V_i(r_i) = \sum_{j=1}^{N_i} \alpha_{ij} \log U_{ij}(r_{ij})$ where $U_{ij}(r_{ij}) > 0$ in accordance with section II utility function properties. Also, logarithmic utilities (equation (2)) concavity stems out $U'_{ij}(r_{ij}) = \frac{dU_{ij}(r_{ij})}{dr_{ij}} > 0$ and $U''_i(r_{ij}) = \frac{d^2 U_{ij}(r_{ij})}{dr_{ij}^2} < 0$, resulting in $\frac{d \log(U_{ij}(r_{ij}))}{dr_{ij}} = \frac{U'_{ij}(r_{ij})}{U_{ij}(r_{ij})} > 0$ due to $U_{ij}(r_{ij}) > 0$ and $U'_{ij}(r_{ij}) > 0$ and in $\frac{d^2 \log(U_{ij}(r_{ij}))}{dr_{ij}^2} = \frac{U''_{ij}(r_{ij})U_{ij}(r_{ij}) - U_{ij}^2(r_{ij})}{U_{ij}^2(r_{ij})} < 0$ due to $U''_{ij}(r_{ij}) < 0$. Thus, the logarithmic utility natural logarithm is strictly concave. On the flip side, for a sigmoidal utility $U_{ij}(r_{ij})$ (equation (1)) with $0 < r_{ij} < R$, we have the following inequalities amongst which the first owes to the sigmoidal function's continuity and $0 \leq U_{ij}(r_{ij}) < 1$ and the rest are utter algebraic manipulation of the first one.

$$\begin{aligned}
0 &< c_{ij} \left(\frac{1}{1 + e^{-a_{ij}(r_{ij}-b_{ij})}} - d_{ij} \right) < 1 \\
d_{ij} &< \frac{1}{1 + e^{-a_{ij}(r_{ij}-b_{ij})}} < \frac{1 + c_{ij}d_{ij}}{c_{ij}} \\
\frac{1}{d_{ij}} &> 1 + e^{-a_{ij}(r_{ij}-b_{ij})} > \frac{c_{ij}}{1 + c_{ij}d_{ij}} \\
0 &< 1 - d_{ij}(1 + e^{-a_{ij}(r_{ij}-b_{ij})}) < \frac{1}{1 + c_{ij}d_{ij}}
\end{aligned}$$

For $0 < r_{ij} < R$, we have the following inequalities, of which the first results from first additive's denominator positivity in addition to the formerly derived statement $0 < 1 - d_{ij}(1 + e^{-a_{ij}(r_{ij}-b_{ij})}) < \frac{1}{1 + c_{ij}d_{ij}}$ as well as other constituents' positivity and the last one is verifiable by investigating its terms algebraically. Hence, the sigmoidal utility natural logarithm is strictly concave. As such, the applications utility functions $U_{ij}(r_{ij}) > 0$ of the system model (equation (3)) have strictly concave natural logarithms, meaning that the aggregated utility $\log V_i(r_i) = \sum_{j=1}^{N_i} \alpha_{ij} \log U_{ij}(r_{ij})$ is strictly concave.

$$\begin{aligned}
\frac{d}{dr_{ij}} \log U_{ij}(r_{ij}) &= \frac{a_{ij}d_{ij}e^{-a_{ij}(r_{ij}-b_{ij})}}{1 - d_{ij}(1 + e^{-a_{ij}(r_{ij}-b_{ij})})} \\
&\quad + \frac{a_{ij}e^{-a_{ij}(r_{ij}-b_{ij})}}{(1 + e^{-a_{ij}(r_{ij}-b_{ij})})} > 0 \\
\frac{d^2}{dr_{ij}^2} \log U_{ij}(r_{ij}) &= \frac{-a_{ij}^2 d_{ij} e^{-a_{ij}(r_{ij}-b_{ij})}}{c_{ij} \left(1 - d_{ij}(1 + e^{-a_{ij}(r_{ij}-b_{ij})}) \right)^2} \\
&\quad + \frac{-a_{ij}^2 e^{-a_{ij}(r_{ij}-b_{ij})}}{(1 + e^{-a_{ij}(r_{ij}-b_{ij})})^2} < 0
\end{aligned} \tag{8}$$

Next, theorem III.2 proves the EURA optimization convexity. ■

Theorem III.2. *The EURA optimization problem in equation (5) is convex and has a unique tractable global optimal solution.*

Proof: The aggregated utility concavity (lemma III.1) concludes the log-EURA (equation (7)) convexity [30], which in turn proves the EURA problem (equation (5)) convexity due to their objective functions equivalence. There exists a unique tractable global optimal solution for a convex optimization [30]. ■

Section III-B explores the IURA optimization convexity.

B. IURA Global Optimal Solution

The IURA objective function $\prod_{j=1}^{N_i} U_{ij}^{\alpha_{ij}}(r_{ij})$ corresponds to $\sum_{j=1}^{N_i} \alpha_{ij} \log(U_{ij}(r_{ij}))$, so equation (6) can be reformulated as equation 9, referred to as the log-IURA problem for which corollary III.3 is conceivable.

$$\begin{aligned}
& \max_{\mathbf{r}_i} \quad \sum_{j=1}^{N_i} \alpha_{ij} \log U_{ij}(r_{ij}) \\
& \text{subject to} \quad \sum_{i=1}^{N_i} r_{ij} \leq r_i^{\text{opt}}, \\
& \quad r_{ij} \geq 0, \quad j = 1, 2, \dots, N_i.
\end{aligned} \tag{9}$$

Corollary III.3. *The IURA optimization problem in equation (6) is convex and has a unique tractable global optimal solution.*

Proof: Substantiating lemma III.1 was concomitant with proving the application utility natural logarithm concavity, which ascertains the convexity of the log-IURA (equation (9)) [30], yielding in the convexity of its equivalent IURA optimization (equation (6)) and existence of a tractable global optimal solution [30]. ■

Theorem III.2 and corollary III.3 indicate that the distributed optimization in section II-D assigns rates optimally. Next, section III-C analyzes the centralized optimization convexity.

C. Centralized Rate Allocation Global Optimal Solution

The centralized optimization objective function $\prod_{i=1}^M \left(\prod_{j=1}^{N_i} U_{ij}^{\alpha_{ij}}(r_{ij}) \right)^{\beta_i}$ corresponds to $\sum_{i=1}^M \beta_i \sum_{j=1}^{N_i} \alpha_{ij} \log U_{ij}(r_{ij})$, reformulating equation (4) as equation 10, referred to as the log-centralized problem, for which corollary III.4 is conceivable.

$$\begin{aligned}
& \max_{\mathbf{r}} \quad \sum_{i=1}^M \beta_i \sum_{j=1}^{N_i} \alpha_{ij} \log U_{ij}(r_{ij}) \\
& \text{subject to} \quad \sum_{i=1}^M \sum_{j=1}^{N_i} r_{ij} \leq R, \\
& \quad r_{ij} \geq 0, \quad i = 1, 2, \dots, M, \quad j = 1, 2, \dots, N_i
\end{aligned} \tag{10}$$

Corollary III.4. *The centralized optimization problem in equation (4) is convex and has a unique tractable global optimal solution.*

Proof: Substantiating lemma III.1 was concomitant with proving the application utility natural logarithm concavity, which entails the the log-centralized optimization (equation (10)) convexity [30], ensuing the convexity of its tantamount centralized optimization (equation (4)) and existence of a tractable global optimal solution [30]. ■

Next, section IV solves the distributed optimization problem presented in section II-D.

IV. EURA ALGORITHM AND DRAWBACK

Here, we deploy the distriduality for convex optimization problems to solving them efficiently, similar to [6], [7]. What proceeds is such an application of the duality to EURA and IURA constituents of the distributed rate allocation problem as well as to the centralized resource assignment problem. We present the EURA algorithm in section IV-A below.

A. EURA Algorithm

The log-EURA problem (7) can be solved by converting it to its dual problem, similar to [6], [7]. We define the Lagrangian as equation (11).

$$\begin{aligned} L(\mathbf{r}, p) &= \sum_{i=1}^M \log(V_i(r_i)) - p \left(\sum_{i=1}^M r_i + \sum_{i=1}^M z_i - R \right) \\ &= \sum_{i=1}^M \left(\log(V_i(r_i)) - pr_i \right) + p \left(R - \sum_{i=1}^M z_i \right) \quad (11) \\ &= \sum_{i=1}^M L_i(r_i, p) + p \left(R - \sum_{i=1}^M z_i \right) \end{aligned}$$

where $z_i \geq 0$ is the slack variable and p is Lagrange multiplier or the shadow price (price per unit bandwidth for all the M channels). Therefore, the i^{th} UE bid for bandwidth can be written as $w_i = pr_i$, where $\sum_{i=1}^M w_i = p \sum_{i=1}^M r_i$. The first term in equation (11) is separable in r_i , so we have $\max_{\mathbf{r}} \sum_{i=1}^M (\log(V_i(r_i)) - pr_i) = \sum_{i=1}^M \max_{r_i} (\log(V_i(r_i)) - pr_i)$ and the dual problem objective function can be written as equation (12).

$$\begin{aligned} D(p) &= \max_{\mathbf{r}} L(\mathbf{r}, p) \\ &= \sum_{i=1}^M \max_{r_i} \left(\log(V_i(r_i)) - pr_i \right) + p \left(R - \sum_{i=1}^M z_i \right) \quad (12) \\ &= \sum_{i=1}^M \max_{r_i} (L_i(r_i, p)) + p \left(R - \sum_{i=1}^M z_i \right) \end{aligned}$$

Thus, the dual problem is formulated as equation (13).

$$\begin{aligned} \min_p \quad & D(p) \\ \text{subject to} \quad & p \geq 0. \end{aligned} \quad (13)$$

Leveraging the method of Lagrange multiplier, we have:

$$\frac{\partial D(p)}{\partial p} = R - \sum_{i=1}^M r_i - \sum_{i=1}^M z_i = 0 \quad (14)$$

Substituting by $\sum_{i=1}^M w_i = p \sum_{i=1}^M r_i$, we have equation (15), minimized to $p = \frac{\sum_{i=1}^M w_i}{R}$ at $\sum_{i=1}^M z_i = 0$ where $w_i = pr_i$ is transmitted by the i^{th} UE to the eNB.

$$p = \frac{\sum_{i=1}^M w_i}{R - \sum_{i=1}^M z_i} \quad (15)$$

As such, we divide the log-EURA problem (7) into simpler optimizations at the eNB (eNB EURA problem) and UEs (UE EURA problem), respectively equations (17) and (16) whose solutions, guaranteeing the utility proportional fairness in equation (5), are summarized in Algorithms IV.2 and IV.1 in that order.

$$\begin{aligned} \max_{r_i} \quad & \log V_i(r_i) - pr_i \\ \text{subject to} \quad & p \geq 0 \\ & r_i \geq 0, \quad i = 1, 2, \dots, M. \end{aligned} \quad (16)$$

During the execution of the aforesaid algorithms, starting with $w_i(0) = 0$, the i^{th} UE, transmits an initial bid $w_i(1)$ to the eNB, which in turn subtracts the latterly received bid $w_i(n)$ and the formerly received one $w_i(n-1)$ and ceases the procedure if the difference is less than a threshold δ ; Otherwise, it computes and sends a shadow price $p(n) = \frac{\sum_{i=1}^M w_i(n)}{R}$ to is covered UEs. The i^{th} UE extracts its rate $r_i(n)$ from the received $p(n)$ such that $\log V_i(r_i) - p(n)r_i$ is maximized. The rate $r_i(n)$ is employed to estimate the new bid $w_i(n) = p(n)r_i(n)$, transmitted to the eNB. This routine repeats until the bid difference $|w_i(n) - w_i(n-1)|$ falls below the threshold δ .

$$\begin{aligned} \min_p \quad & D(p) \\ \text{subject to} \quad & p \geq 0. \end{aligned} \quad (17)$$

The solution $r_i(n)$ of the i^{th} UE EURA optimization $r_i(n) = \arg \max_{r_i} (\log V_i(r_i) - p(n)r_i)$ in Algorithm IV.1 essentially solves the equation $\frac{\partial \log V_i(r_i)}{\partial r_i} = p(n)$, algebraically the Lagrange multiplier solution for equation (16) and geometrically the intersection point of the horizontal line $y = p(n)$ with the curve $y = \frac{\partial \log V_i(r_i)}{\partial r_i}$.

A convergence analysis of the EURA algorithms and its resultant snags are discussed in section IV-B.

B. EURA Convergence Analysis

To commence analyzing the EURA Algorithms IV.1 and IV.2, lemma IV.1 is envisaged.

Lemma IV.1. *The aggregated utility function $V_i(r_i)$, the slope curvature function $\frac{\partial \log V_i(r_i)}{\partial r_i}$ has inflection points at $r_i = r_{ij}^s \approx r_{ij}^{inf}$ for j^{th} application utility function U_{ij} and is convex for $r_{ij} > \max_j r_{ij}^s$.*

Algorithm IV.1 UE EURA Optimization

Send initial bid $w_i(1)$ to eNB.
loop
 Receive shadow price $p(n)$ from eNB.
if STOP from eNB **then**
 Calculate allocated rate $r_i^{\text{opt}} = \frac{w_i(n)}{p(n)}$.
 STOP
else
 Solve $r_i(n) = \arg \max_{r_i} (\log V_i(r_i) - p(n)r_i)$.
 Send new bid $w_i(n) = p(n)r_i(n)$ to eNB.
end if
end loop

Algorithm IV.2 eNB EURA Optimization

loop
 Receive bids $w_i(n)$ from UEs. {Let $w_i(0) = 1 \ \forall i$ }
if $|w_i(n) - w_i(n-1)| < \delta \ \forall i$ **then**
 Allocate rates, $r_i^{\text{opt}} = \frac{w_i(n)}{p(n)}$ to user i .
 STOP
else
 Calculate $p(n) = \frac{\sum_{i=1}^M w_i(n)}{R}$.
 Send new shadow price $p(n)$ to all UEs.
end if
end loop

Proof: For the i^{th} UE aggregated utility $V_i(r_i)$, let $S_i(r_i) = \frac{\partial \log V_i(r_i)}{\partial r_i}$ be the aggregated utility slope curvature function, $S_{ij}(r_{ij}) = \frac{\partial \log U_{ij}(r_{ij})}{\partial r_{ij}}$ be the j^{th} application utility slope curvature function, and N_i^S be the number of sigmoidal utilities. Taking the logarithm and derivative of both sides of the equation (3) yields in equation (18).

$$\begin{aligned}
 S_i(r_i) &= \frac{\partial \log V_i(r_i)}{\partial r_i} = \frac{\partial}{\partial r_i} \sum_{j=1}^{N_i} \alpha_{ij} \log U_{ij}(r_{ij}) \\
 &= \sum_{j=1}^{N_i} \alpha_{ij} \frac{\partial \log U_{ij}(r_{ij})}{\partial r_{ij}} = \sum_{j=1}^{N_i} \alpha_{ij} S_{ij}(r_{ij}) \quad (18) \\
 &= \sum_{j=1}^{N_i^S} \alpha_{ij} S_{ij}(r_{ij}) + \sum_{j=N_i^S+1}^{N_i} \alpha_{ij} S_{ij}(r_{ij})
 \end{aligned}$$

Taking the 1^{th} and 2^{nd} derivatives of equation (18), we write:

$$\begin{aligned}
 \frac{\partial S_i}{\partial r_i} &= \sum_{j=1}^{N_i^S} \left\{ \frac{-\alpha_{ij} a_{ij}^2 d_{ij} e^{-a_{ij}(r_{ij}-b_{ij})}}{c_{ij} \left(1 - d_{ij} (1 + e^{-a_{ij}(r_{ij}-b_{ij})})\right)^2} \right. \\
 &\quad \left. + \frac{\alpha_{ij} a_{ij}^2 e^{-a_{ij}(r_{ij}-b_{ij})}}{(1 + e^{-a_{ij}(r_{ij}-b_{ij})})^2} \right\} \\
 &\quad - \sum_{j=N_i^S+1}^{N_i} \left\{ \frac{\alpha_{ij} k_{ij}^2}{(1 + k_{ij} r_{ij})^2 \log(1 + k_{ij} r_{ij})} \right\} \quad (19)
 \end{aligned}$$

$$\begin{aligned}
 \frac{\partial^2 S_i}{\partial r_i^2} &= \sum_{j=1}^{N_i^S} \left\{ \frac{d_{ij} e^{-a_{ij}(r_{ij}-b_{ij})} (1 - d_{ij} (1 - e^{-a_{ij}(r_{ij}-b_{ij})}))}{c_{ij} \left(1 - d_{ij} (1 + e^{-a_{ij}(r_{ij}-b_{ij})})\right)^3} \right. \\
 &\quad \left. + \frac{e^{-a_{ij}(r_{ij}-b_{ij})} (1 - e^{-a_{ij}(r_{ij}-b_{ij})})}{(1 + e^{-a_{ij}(r_{ij}-b_{ij})})^3} \right\} \times a_{ij}^3 \alpha_{ij} \\
 &\quad - \sum_{j=N_i^S+1}^{N_i} \left\{ \frac{\alpha_{ij} k_{ij}^2 (\log(1 + k_{ij} r_{ij}) - 1)}{(1 + k_{ij} r_{ij})^2 \log^2(1 + k_{ij} r_{ij})} \right\} \quad (20)
 \end{aligned}$$

It is easy to show that $\forall r_i, \frac{\partial S_i}{\partial r_i} < 0$. Denoting the 1^{th} term of equation (19) and 2^{nd} and 3^{rd} terms of equation (20) as respectively S_i^1 , S_i^2 , and S_i^3 stems out equation set (21), for which properties in equation set (22) are considerable.

$$\begin{cases} S_i^1 = \frac{\alpha_{ij} a_{ij}^3 e^{a_{ij} b_{ij}} (e^{a_{ij} b_{ij}} + e^{-a_{ij}(r_{ij}-b_{ij})})}{(e^{a_{ij} b_{ij}} - e^{-a_{ij}(r_{ij}-b_{ij})})^3} \\ S_i^2 = \frac{a_{ij}^3 \alpha_{ij} e^{-a_{ij}(r_{ij}-b_{ij})} (1 - e^{-a_{ij}(r_{ij}-b_{ij})})}{(1 + e^{-a_{ij}(r_{ij}-b_{ij})})^3} \\ S_i^3 = \frac{\alpha_{ij} k_{ij}^2 (\log(1 + k_{ij} r_{ij}) - 1)}{(1 + k_{ij} r_{ij})^2 \log^2(1 + k_{ij} r_{ij})} \end{cases} \quad (21)$$

From equation set (22), we observe that the slope curvature function S_i has the inflection point $r_i = r_{ij}^s \approx b_{ij} = r_{ij}^{\text{inf}}$ and changes from a convex function close to the origin to a concave function before the inflection point at $r_{ij} = r_{ij}^s$ to a convex function after the inflection point.

$$\begin{cases} \lim_{r_i \rightarrow 0} S_i^1 = \infty, \\ \lim_{r_i \rightarrow b_{ij}} S_i^1 = 0 \text{ for } b_{ij} \gg \frac{1}{a_{ij}} \ \forall j \\ S_i^2(b_{ij}) = 0 \\ S_i^2(r_{ij} > b_{ij}) > 0 \\ S_i^2(r_{ij} < b_{ij}) < 0 \\ S_i^3(r_{ij} > 0) > 0 \end{cases} \quad (22)$$

Corollary IV.2. If $\sum_{i=1}^M \max_j r_{ij}^s \ll R$, then Algorithms IV.1 and IV.2 converge to the global optimal rates corresponding to the steady state shadow price $p_{ss} < \frac{a_{i_{\max}} d_{i_{\max}}}{1 - d_{i_{\max}}} + \frac{a_{i_{\max}}}{2}$, where $i_{\max} = \arg \max_i r_{ij_{\max}}^s$ and $r_{ij_{\max}}^s = \max_j r_{ij}^s$.

Proof: An essential step to reach the optimal solution in Algorithm (IV.1) is solving $r_i(n) = \arg \max_{r_i} (\log V_i(r_i) - p(n)r_i)$ using the Lagrange multipliers in equation (23).

$$\frac{\partial \log V_i(r_i)}{\partial r_i} - p = S_i(r_i) - p = 0. \quad (23)$$

Furthermore, equation set (22) indicate that the slope curvature function $S_i(r_i)$ is convex for $r_i > \max_j r_{ij}^s \approx \max_j b_{ij}$. Similar to the analyses in [6], [7], the Algorithms IV.1 and IV.2 are guaranteed to converge to the global optimal solution when the aggregated slope curvature function $S_i(r_i)$ is in the convex region. Hence, the aggregated utility natural logarithm converges to the global optimal solution for $r_i > \max_j r_{ij}^s \approx \max_j b_{ij}$. On the other hand, the sigmoidal utility function

inflection point is at $r_i^{\text{inf}} = b_{ij}$. For $\sum_{i=1}^M \max_j r_{ij}^s \ll R$, Algorithms IV.1 and IV.2 allocate rates $r_{ij} > b_{ij}$ for all users and since $S_{ij}(r_{ij})$ is convex for $r_{ij} > r_{ij}^s \approx b_{ij}$, the optimal solution can be achieved by the algorithms. Equation (23) and convexity of $S_{ij}(r_{ij})$ for $r_{ij} > r_{ij}^s \approx b_{ij}$ imply that $p_{ss} < S_{ij}(r_{ij} = \max b_{ij})$, where $S_{ij}(r_{ij} = \max b_{ij}) = \frac{a_{i\max} d_{i\max}}{1-d_{i\max}} + \frac{a_{i\max}}{2}$ and $i_{\max} = \arg \max_i b_{ij}$. ■

Corollary IV.3. For $\sum_{i=1}^M \max_j r_{ij}^s > R$ and the global optimal shadow price $p_{ss} \approx \frac{a_{ij} d_{ij} e^{\frac{a_{ij} b_{ij}}{2}}}{1-d_{ij}(1+e^{\frac{a_{ij} b_{ij}}{2}})} + \frac{a_{ij} e^{\frac{a_{ij} b_{ij}}{2}}}{(1+e^{\frac{a_{ij} b_{ij}}{2}})}$, the solution by EURA Algorithms IV.1 and IV.2 fluctuates about the global optimal solution.

Proof: It follows from lemma IV.1 that for $\sum_{i=1}^M r_{ij}^{\text{inf}} > R$, $\exists i$ such that the optimal rates $r_{ij}^{\text{opt}} < b_{ij}$. Thus, $p_{ss} \approx \frac{a_{ij} d_{ij} e^{\frac{a_{ij} b_{ij}}{2}}}{1-d_{ij}(1+e^{\frac{a_{ij} b_{ij}}{2}})} + \frac{a_{ij} e^{\frac{a_{ij} b_{ij}}{2}}}{(1+e^{\frac{a_{ij} b_{ij}}{2}})}$ is the optimal shadow price for the optimization problem in equation (5). Then, a small change in the shadow price $p(n)$ at the n^{th} iteration can cause the rate $r_{ij}(n)$ (the root of $S_{ij}(r_{ij}) - p(n) = 0$) to fluctuate between the concave and convex curvature of the slope curve $S_{ij}(r_{ij})$ for the i^{th} UE. Therefore, it produces a fluctuation in the bid value $w_i(n)$ sent to the eNB, which in turn induces a vacillation of the shadow price $p(n)$ transmitted by eNB to the UEs. Hence, the iterative solution oscillates about the global optimal rates r_{ij}^{opt} . ■

Theorem IV.4. EURA Algorithms IV.1 and IV.2 do not converge to the optimal solution for all eNB rates R .

Proof: It directly follows from the corollaries IV.2 and IV.3 that the EURA algorithm does not converge to the global optimal solution for all values of R . ■

The potential EURA seesawing about optimal rates and dearth of convergence thereof motivate us to include some robustness into the procedure. This is done in section IV-C.

C. EURA Robust Algorithm

Incorporate robustness into the EURA Algorithms IV.1 and IV.2 so that they converge for all eNB rates requires the algorithm to refrain from fluctuations in the non-convergent region for $\sum_{i=1}^M \max_j r_{ij}^s \ll R$. To do this, a fluctuation decay function $\Delta w(n)$ as below reduces the step size between the current and previous bid, i.e. $w_i(n) - w_i(n-1)$, for every user i if a fluctuation occurs. The allocated rates should coincide with the those of EURA Algorithms IV.1 and IV.2 for $\sum_{i=1}^M \max_j r_{ij}^s > R$.

- Exponential function: $\Delta w(n) = l_1 e^{-\frac{n}{l_2}}$.
- Rational function: $\Delta w(n) = \frac{l_3}{n}$.

where l_1, l_2, l_3 can be adjusted to change the bids w_i decay rate.

Remark IV.5. The fluctuation decay function can be included in either UE EURA Algorithm or eNB EURA Algorithm.

In our model, we choose to incorporate the decay function into the UE EURA Algorithm even though, as mentioned

before, it can be placed in the eNB EURA as well. The fledgling robust EURA process is illustrated in Algorithms IV.3 and IV.4. Here, starting with $w_i(0) = 0$, each UE commences transmitting an initial bid $w_i(1)$ to the eNB, which at each iterate n calculates the difference between the currently and formerly received bids $w_i(n)$ and $w_i(n-1)$, then exits if the difference falls below a threshold δ ; otherwise, it computes the shadow price $p_E(n) = \frac{\sum_{i=1}^M w_i(n)}{R}$ and send it to its covered UEs, amongst which The i^{th} UE obtains the rate r_i maximizing the statement $\log \beta_i V_i(r_i) - p_E(n) r_i$, estimates its new bid $w_i(n) = p_E(n) r_i(n)$, and sends it to the eNB.

Algorithm IV.3 UE Robust EURA Algorithm

Send initial bid $w_i(1)$ to eNB.

loop

Receive shadow price $p(n)$ from eNB.

if STOP from eNodeB **then**

Calculate allocated rate $r_{ij}^{\text{opt}} = \frac{w_i(n)}{p(n)}$.

else

Solve $r_i(n) = \arg \max_{r_i} (\beta_i \log V_i(r_i) - p_E(n) r_i)$.

Calculate new bid $w_i(n) = p(n) r_i(n)$.

if $|w_i(n) - w_i(n-1)| > \Delta w(n)$ **then**

$w_i(n) = w_i(n-1) + \text{sign}(w_i(n) - w_i(n-1)) \Delta w(n)$
 $\{\Delta w = l_1 e^{-\frac{n}{l_2}} \text{ or } \Delta w = \frac{l_3}{n}\}$

end if

Send new bid $w_i(n)$ to eNB.

end if

end loop

Algorithm IV.4 eNB EURA Algorithm

loop

Receive bids $w_i(n)$ from UEs {Let $w_i(0) = 1 \forall i$ }

if $|w_i(n) - w_i(n-1)| < \delta \forall i$ **then**

STOP and allocate rates (i.e r_i^{opt} to user i)

else

Calculate $p_E(n) = \frac{\sum_{i=1}^M w_i(n)}{R}$

Send new shadow price $p_E(n)$ to all UEs

end if

end loop

Remark IV.6. If the subscriber differentiation parameter β_i is available only at the eNB (or other network provider unit), the shadow price p_E is changed to $\frac{p_E}{\beta_i}$.

D. IURA Algorithm

This section presents the second stage of the distributed resource allocation during which the application rates r_{ij} are optimally assigned internally to the UEs in accordance with Algorithm IV.5, where the i^{th} UE leverages the EURA allocated rate r_i^{opt} to solve $\mathbf{r}_i = \arg \max_{\mathbf{r}_i} \sum_{j=1}^{N_i} (\alpha_{ij} \log U_{ij}(r_{ij}) - p_I r_{ij}) + p_I r_{ij}^{\text{opt}}$.

Next, section V includes the centralized resource allocation algorithm in which the application rate are assigned in a monolithic stage.

Algorithm IV.5 UE IURA Optimization

```

loop
  Receive  $r_i^{\text{opt}}$  from eNB. {by EURA Algorithms}
  Solve
   $\mathbf{r}_i = \arg \max_{\mathbf{r}_i} \sum_{j=1}^{N_i} (\alpha_{ij} \log U_{ij}(r_{ij}) - p_I r_{ij}) + p_I r_i^{\text{opt}}$ 
   $\{\mathbf{r}_i = \{r_{i1}, r_{i2}, \dots, r_{iN_i}\}\}$ 
  Allocate  $r_{ij}$  to the  $j^{\text{th}}$  application.
end loop
  
```

V. CENTRALIZED ALGORITHM

The process for the centralized resource allocation (4) consists of UE and eNB parts shown in respectively Algorithms V.1 and V.2, whose executions (Figure 2) start by UEs transmitting their application utility parameters to the eNB, which in turn solves the entire optimization by allotting the bandwidth to the applications in an optimum fashion. The rates, solutions to equation (III-C), are the values r_{ij} which solve the equation $\frac{\partial \log U_{ij}(r_{ij})}{\partial r_{ij}} = p(n)$ and are the intersection of the time varying shadow price, horizontal line $y = p(n)$, with the curve $y = \frac{\partial \log U_{ij}(r_{ij})}{\partial r_{ij}}$ geometrically.

Algorithm V.1 UE Centralized Algorithm

```

loop
  Send application utility parameters
   $\{a_{ij}, b_{ij}, \alpha_{ij}, k_{ij}, r_{ij}^{\text{max}}\}$  to eNB.
  Receive rates  $r_i^{\text{opt}} = \{r_{i1}^{\text{opt}}, r_{i2}^{\text{opt}}, \dots, r_{iN_i}^{\text{opt}}\}$  from eNB.
  Allocate rate  $r_{ij}^{\text{opt}}$  internally to  $j^{\text{th}}$  applications.
end loop
  
```

Algorithm V.2 eNB Centralized Algorithm

```

loop
  Receive application utility parameters
   $\{a_{ij}, b_{ij}, \alpha_{ij}, k_{ij}, r_{ij}^{\text{max}}\}$  from UEs.
  Solve  $\mathbf{r} = \arg \max_{\mathbf{r}} \sum_{i=1}^M \beta_i \sum_{j=1}^{N_i} \alpha_{ij} \log U_{ij}(r_{ij}) - p(\sum_{i=1}^M \sum_{j=1}^{N_i} r_{ij} - R)$ . {where  $\mathbf{r} = \{r_1, r_2, \dots, r_M\}$  and  $r_i = \{r_{i1}, r_{i2}, \dots, r_{iN_i}\}$ }
  Send  $r_i = \{r_{i1}, r_{i2}, \dots, r_{iN_i}\}$  to  $i^{\text{th}}$  UE.
end loop
  
```

Section VI proves that the distributed and centralized resource allocation methods are equivalent.

VI. EQUIVALENCE

Here, we show the mathematical equivalence of the distributed resource allocation in equations (5) and (6) with the centralized approach in equation (4). First, lemma VI.1 is conceivable.

Lemma VI.1. *The aggregated and application utility slope curvature functions $S_i(r_i) = \frac{\partial \log V_i(r_i)}{\partial r_i}$ and $S_{ij}(r_{ij}) = \frac{\partial \log U_{ij}(r_{ij})}{\partial r_{ij}}$ are invertible and their inverse functions $r_i = S_i^{-1}(\cdot)$ and $r_{ij} = S_{ij}^{-1}(\cdot)$ are strictly decreasing.*

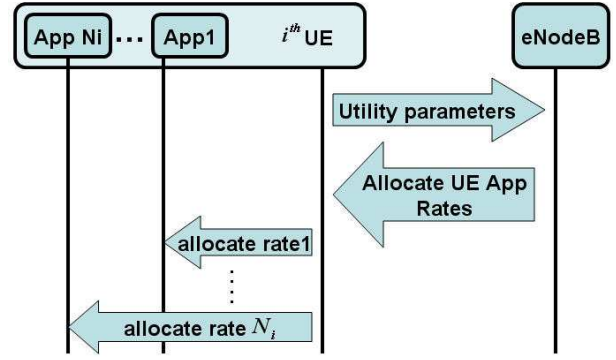


Fig. 2. Centralized Algorithm: Resources are allocated to the applications running on the UEs in a monolithic stage, in which UEs transmit their application utility parameters to their eNB, which calculates the optimal application rates and transmit them to the germane UEs.

Proof: The concavity of the logarithmic utility U_{ij} yields in $U'_{ij}(r_{ij}) = \frac{\partial U_{ij}(r_{ij})}{\partial r_{ij}} > 0$ and $U''_{ij}(r_{ij}) = \frac{\partial^2 U_{ij}(r_{ij})}{\partial r_{ij}^2} < 0$, and lemma III.1 stems out $S_{ij}(r_{ij}) = \frac{\partial \log(U_{ij}(r_{ij}))}{\partial r_{ij}} = \frac{U'_{ij}(r_{ij})}{U_{ij}(r_{ij})} > 0$ and $\frac{\partial S_{ij}(r_{ij})}{\partial r_{ij}} = \frac{U''_{ij}(r_{ij})U_{ij}(r_{ij}) - U_{ij}'^2(r_{ij})}{U_{ij}^2(r_{ij})} < 0$. Also, for the utility function, we have $U_{ij}(r_{ij}) > 0$, $U_{ij}(r_{ij})$ is increasing, and it is twice differentiable with respect to r_{ij} (section II). Therefore, $S_{ij}(r_{ij})$ of the logarithmic utility function is strictly decreasing. From equation (24), for the sigmoidal utility function $U_{ij}(r_{ij})$ where $0 < r_{ij} < R$, we can write inequality set (24), giving that $S_{ij}(r_{ij})$ of the sigmoidal utility function is strictly decreasing.

$$S_{ij}(r_{ij}) > 0, \frac{\partial}{\partial r_{ij}} S_{ij}(r_{ij}) < 0 \quad (24)$$

Equation (18) and inequalities 24 yield in inequalities (25). Henceforth, $S_{ij}(r_{ij})$ and $S_i(r_i)$ of all the utilities in section II are strictly decreasing functions; thereby, the slope curvature functions $S_{ij}(r_{ij})$ and $S_i(r_i)$ are invertible and the inverse functions are strictly decreasing.

$$\begin{aligned}
 S_i(r_i) &= \sum_{j=1}^{N_i^S} \alpha_{ij} S_{ij}(r_{ij}) + \sum_{j=N_i^S+1}^{N_i} \alpha_{ij} S_{ij}(r_{ij}) > 0 \\
 \frac{\partial S_i(r_i)}{\partial r_i} &= \sum_{j=1}^{N_i^S} \alpha_{ij} \frac{\partial S_{ij}(r_{ij})}{\partial r_{ij}} + \sum_{j=N_i^S+1}^{N_i} \alpha_{ij} \frac{\partial S_{ij}(r_{ij})}{\partial r_{ij}} < 0
 \end{aligned} \quad (25)$$

Corollary VI.2. *The optimal rates assigned by the distributed optimization in equations (5) and (6) is equal to the one allocated by the centralized optimization in equation (4).*

Proof: The centralized optimization's (equation(10)) lagrangian can be written as equation (26) where $z \geq 0$ is the slack variable and p_T is the lagrange multiplier.

$$L_T(\mathbf{r}) = \left(\sum_{i=1}^M \beta_i \sum_{j=1}^{N_i} \alpha_{ij} \log U_{ij}(r_{ij}) \right) - p_T \left(\sum_{i=1}^M \sum_{j=1}^{N_i} r_{ij} - R + z \right) \quad (26)$$

Then, we have that:

$$\frac{\partial L_T(\mathbf{r})}{\partial r_{ij}} = \beta_i \alpha_{ij} S_{ij}(r_{ij}) - p_T = 0 \Rightarrow p_T = \beta_i \alpha_{ij} S_{ij}(r_{ij}) \quad (27)$$

so, the i^{th} UE's j^{th} application rate is:

$$r_{ij} = S_{ij}^{-1} \left(\frac{p_T}{\beta_i \alpha_{ij}} \right) \quad (28)$$

Using equation (18), we can write:

$$N_i p_T = \beta_i S_i(r_i) \quad (29)$$

And the i^{th} UE rate can be calculated as equation (30).

$$r_i = S_i^{-1} \left(\frac{N_i p_T}{\beta_i} \right). \quad (30)$$

The EURA optimization's (equation (7)) lagrangian can be written as equation (31) where $z \geq 0$ is the slack variable and p_E is the lagrange multiplier.

$$L_E(\mathbf{r}) = \left(\sum_{i=1}^M \beta_i \log V_i(r_i) \right) - p_E \left(\sum_{i=1}^M r_i - R + z \right) \quad (31)$$

Then, we have that:

$$\frac{\partial L_E(\mathbf{r})}{\partial r_i} = \beta_i S_i(r_i) - p_E = 0 \Rightarrow p_E = \beta_i S_i(r_i) \quad (32)$$

So, the i^{th} UE rate is:

$$r_i = S_i^{-1} \left(\frac{p_E}{\beta_i} \right) \quad (33)$$

Replacing S_i from equation (18), we can write:

$$p_E = \beta_i \sum_{j=1}^{N_i} \alpha_{ij} S_{ij}(r_{ij}) \quad (34)$$

And, we get equation (35) below.

$$p_E = \sum_{j=1}^{N_i} p_T = N_i p_T \quad (35)$$

Equations (30) and (33) signify that the centralized and EURA optimizations lead to identical UE rates.

The IURA optimization's (equation 9) lagrangian can be written as equation (36) where $z \geq 0$ is the slack variable and p_I is the lagrange multiplier corresponding to the internal shadow price, price per bandwidth for all applications in the i^{th} UE.

$$L_I(r_i) = \left(\sum_{j=1}^{N_i} \alpha_{ij} \log U_{ij}(r_{ij}) \right) - p_I \left(\sum_{j=1}^{N_i} r_{ij} - r_{ij}^{\text{opt}} + z \right) \quad (36)$$

Then, we have that:

$$\frac{\partial L_I(r_i)}{\partial r_{ij}} = \alpha_{ij} S_{ij}(r_{ij}) - p_I = 0 \Rightarrow p_I = \alpha_{ij} S_{ij}(r_{ij}) \forall j \quad (37)$$

And, summing the i^{th} UE applications gives that:

$$\sum_{j=1}^{N_i} p_I = \sum_{j=1}^{N_i} \alpha_{ij} S_{ij}(r_{ij}) \quad (38)$$

Using equation (18) results in equation (39).

$$\beta_i N_i p_I = \beta_i S_i(r_i) = p_E = N_i p_T \Rightarrow p_T = \beta_i p_I \quad (39)$$

So, i^{th} UE's j^{th} application rate can be written as equation (39).

$$r_{ij} = S_{ij}^{-1} \left(\frac{p_I}{\alpha_{ij}} \right) = S_{ij}^{-1} \left(\frac{p_T}{\beta_i \alpha_{ij}} \right) \quad (40)$$

Considering the constraints of the equation (9), the total rate of the i^{th} UE can be written as equation (41).

$$r_i^{\text{opt}} = \sum_{j=1}^{N_i} r_{ij} = \sum_{j=1}^{N_i} S_{ij}^{-1} \left(\frac{p_T}{\beta_i \alpha_{ij}} \right) \quad (41)$$

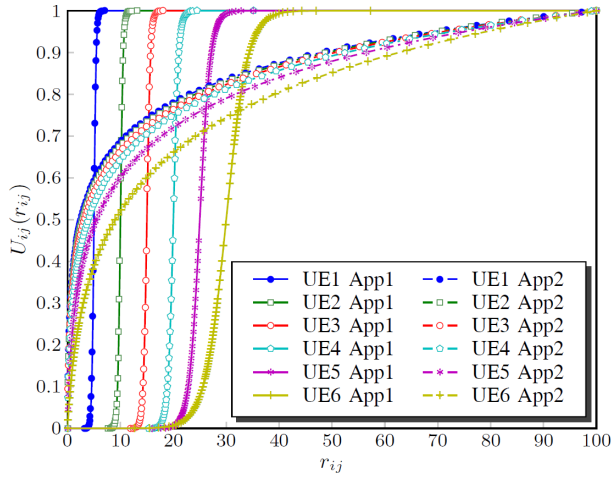
Equations (40) and (39) signify that the centralized and IURA optimizations lead to identical application rates. As such, the UE and application rates assigned by the centralized and distributed optimizations are the same. ■

Theorem VI.3. *The distributed optimization in equations (5) and (6) is equivalent to the centralized optimization in equation (4).*

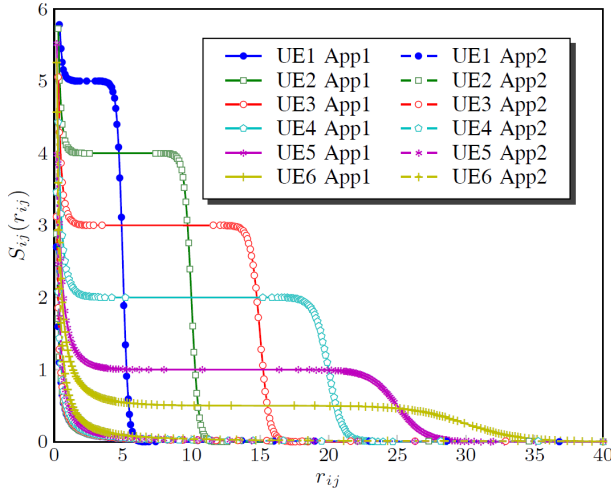
Proof: Stemming out equal rates (Corollary VI.2) indicates the distributed and centralized optimizations are equivalent. ■

VII. SIMULATION RESULTS

A cell with $M = 6$ UEs and an eNB, depicted in Figure 1, is considered and each UE concurrently runs a delay-tolerant and a real-time application with respectively logarithmic and sigmoidal utility functions with parameters in Table I. The sigmoidal utility with parameters $a = 5$, $b = 10$ approximates a step function at rate $r = 5$ and is a good model for Voice-over-IP (VoIP), while parameters $a = 3$, $b = 15$ is an approximation of a real-time application with an inflection point at rate $r = 15$ and is conducive to modeling standard definition video streaming, whereas parameters $a = 1$, $b = 25$ is an estimation of another real-time application with the inflection point $r = 25$ and is appropriate for the high definition video streaming. Moreover, the logarithmic utilities with $r^{\text{max}} = 100$ and distinct k_i parameters estimate delay-tolerant FTP applications. The plots of the utility functions in Table I are shown in Figure ??, from which we can observe that the real-time applications require a minimum rate, i.e. the inflection point, after which the application QoS is fulfilled to a large extent. On the other hand, the logarithmic utility is provided with some QoS even at low rates suitable for the



(a) Application Utility Functions

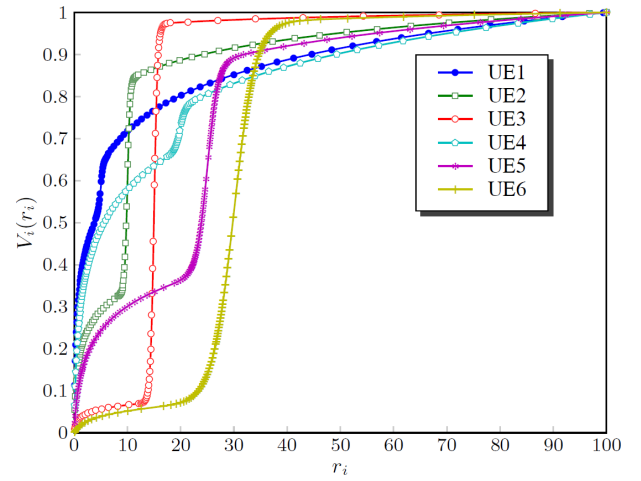


(b) Utility Slope Curvature Functions

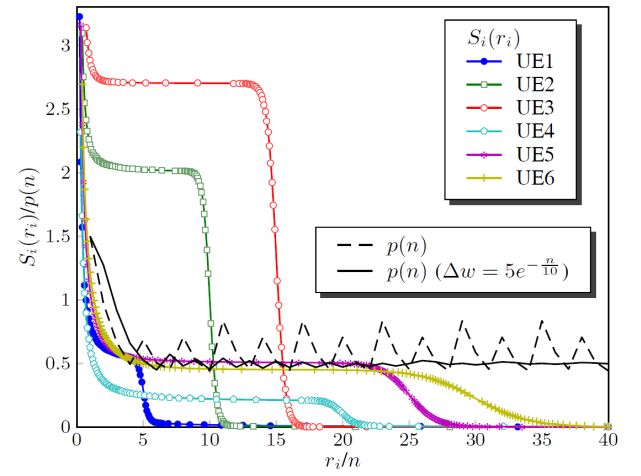
Fig. 3. The system contains 6 UEs, each concurrently running a delay-tolerant and real-time application with respective identically colored logarithmic and sigmoidal utility functions U_{ij} vs. the application-assigned rates r_{ij} plots in Figure 3(a). Utility slope curvature functions, the first derivative of the application utility natural logarithms S_{ij} with respect to the application rates r_{ij} are illustrated in Figure 3(b) where identical colors relate to the applications on one UE.

delay-tolerant nature of the applications. Furthermore, as we can observe from Figure 3(a), in compliance with the properties mentioned in section II the utility functions are strictly increasing continuous functions, zero valued at zero rates. Furthermore, the first derivative of the utility functions natural logarithm, $S_{ij}(r_{ij})$, are shown in Figure 3(b), which reflects the positivity and decreasing nature of the first derivative in line with lemmas VI.1 and VI.1.

Then, the distributed resource allocation approach (Algorithms IV.3, IV.4, and IV.5) and the centralized rate assignment procedure (Algorithms V.1 and V.2) were applied to the aforesaid logarithmic and sigmoidal utility functions using MATLAB. To account for the applications usage percentage, we set the application status weight vector in equation (3) as $\alpha = \{\alpha_{11}, \alpha_{21}, \alpha_{31}, \alpha_{41}, \alpha_{51}, \alpha_{61}, \alpha_{12}, \alpha_{22}, \alpha_{32}, \alpha_{42}, \alpha_{52}, \alpha_{62}\}$ where α_{ij} represents the status weight of the j^{th} application



(a) Aggregated Utility Functions



(b) Aggregated Slope Curvature Functions

Fig. 4. Figure 4(a) plots the aggregated utilities, multiplications of the usage-percentage-powered application utility functions $V_i(r_i)$ vs. the UE rates r_i , where $i \in \{1, \dots, 6\}$. Figure 4(b) illustrates the aggregated slope curvature functions, first derivative of the aggregated utility natural logarithms $S_i(r_i)$. Furthermore, decay function-induced robustness effect is depicted; As we can see, the lack of decay functions yields in the system instability revealed in the shadow price oscillation.

of the i^{th} UE. It is noteworthy that the addition of application usage percentages per UE is unity, i.e. $\alpha_{i1} + \alpha_{i2} = 1$.

In addition, the aggregated utility functions $V_i(r_i)$ for $i \in \{1, \dots, 6\}$ are depicted in Figure 4(a) and the first derivative of their natural logarithm, $S_i(r_i)$ for $i \in \{1, \dots, 6\}$, are illustrated in Figure 4(b). As we can see, in compliance with lemma IV.1, the slope curvature functions inflection points occur at the application utility functions' inflection points. Furthermore, in line with lemma VI.1, the slope curvature functions are strictly decreasing.

Next section investigates bids and rate allocations for the UEs and applications in our system under varying eNB resource availabilities.

A. Rate Allocation and Bids for $10 \leq R \leq 200$

In the following simulations, we set the termination threshold $\delta = 10^{-4}$ and the eNB rate R to sweep from

TABLE I
APPLICATIONS UTILITY PARAMETERS

Applications Utilities Parameters	
UE1 App1	Sigmoid $a = 5$, $b = 5$
UE2 App1	Sigmoid $a = 4$, $b = 10$
UE3 App1	Sigmoid $a = 3$, $b = 15$
UE4 App1	Sigmoid $a = 2$, $b = 20$
UE5 App1	Sigmoid $a = 1$, $b = 25$
UE6 App1	Sigmoid $a = 0.5$, $b = 30$
UE1 App2	Logarithmic $k = 15$, $r^{\max} = 100$
UE2 App2	Logarithmic $k = 12$, $r^{\max} = 100$
UE3 App2	Logarithmic $k = 9$, $r^{\max} = 100$
UE4 App2	Logarithmic $k = 6$, $r^{\max} = 100$
UE5 App2	Logarithmic $k = 3$, $r^{\max} = 100$
UE6 App2	Logarithmic $k = 1$, $r^{\max} = 100$

10 to 200 with an step size of 5 bandwidth units. Besides, the application status weights is considered to be $\alpha = \{0.1, 0.5, 0.9, 0.1, 0.5, 0.9, 0.9, 0.5, 0.1, 0.9, 0.5, 0.1\}$. It is worth mentioning that the addition of usage percentages per UE is unity, e.g. adding the 1st and the 6th components of the set (which are indeed the usage percentages for both of applications running on UE1), we get $0.1 + 0.9 = 1$, and so forth. For the distributed resource allocation (Algorithms IV.3, IV.4, and IV.5), UE assigned rates and pledged bids are depicted in Figure 5(a) during the EURA Algorithm with the changes in the eNB available resources R . As we can observe, initially all the UEs are allocated some rates which is owing to the fact that they all subsume real-time applications in need of immediate rate allocations before any QoS is met. For instance, UE2 has a real-time streaming video application (based on Table I), which requires a bandwidth assignment right away. In Figure 5(b), we show the UEs bids $\{w_i | i \in \{1, \dots, 6\}\}$ during the EURA algorithm under changing eNB bandwidth R . First of all, we see that the more resources become available at the eNB, the higher rates are assigned to the UEs. On the other hand, the dearth of the resources (small R) causes those UEs which have applications with higher bit rate requirements to bid higher in order to gain resources. For instance, since UE2 includes a real-time streaming video application, its urgent need for bandwidth allocation causes its initial higher bid for the resources, which is responded by its fast allocation portrayed in the Figure 5(a).

Then, the IURA algorithm has the UEs internally allocate rates to their applications based on the pledged bids as illustrated in Figures 6(a) and 6(b). In Figure 6(a), we show the allocated applications rates $\{r_{ij} | i \in \{1, \dots, 6\} \wedge j \in \{1, 2\}\}$ during the IURA algorithm under changing eNB rate R . As we can observe, initially more resources are allocated to the real-time applications since these have more stringent QoS requirements. In Figure 6(b), we illustrate the applications' internally pledged bids $\{w_{ij} | i \in \{1, \dots, 6\} \wedge j \in \{1, 2\}\}$ during the IURA algorithm under changing eNB rate R . Inasmuch as the real-time applications of the UEs need more resources, they bid higher than the delay-tolerant applications specially

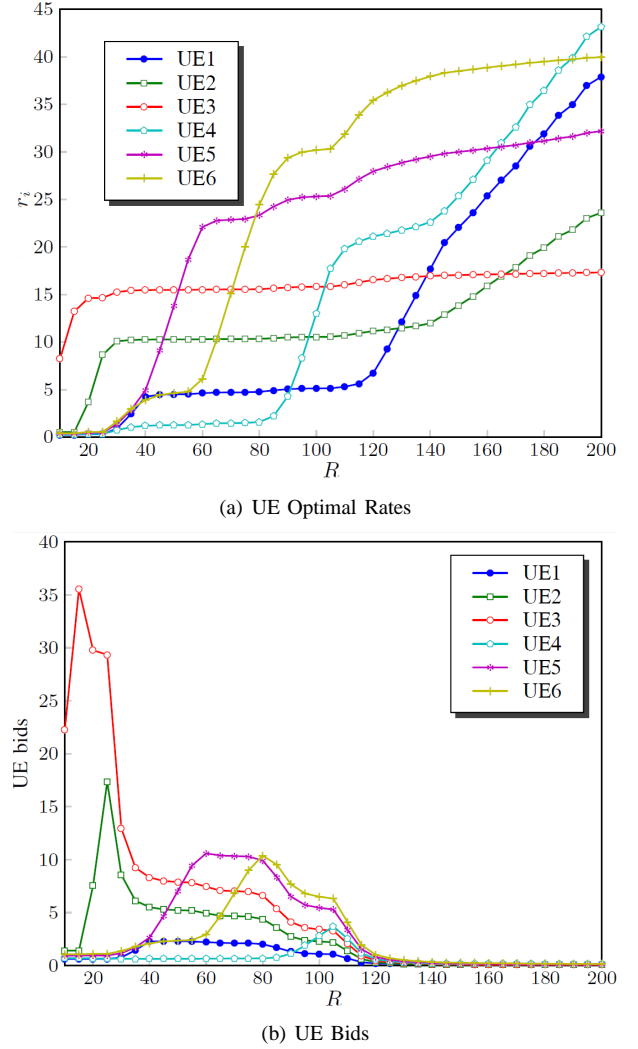
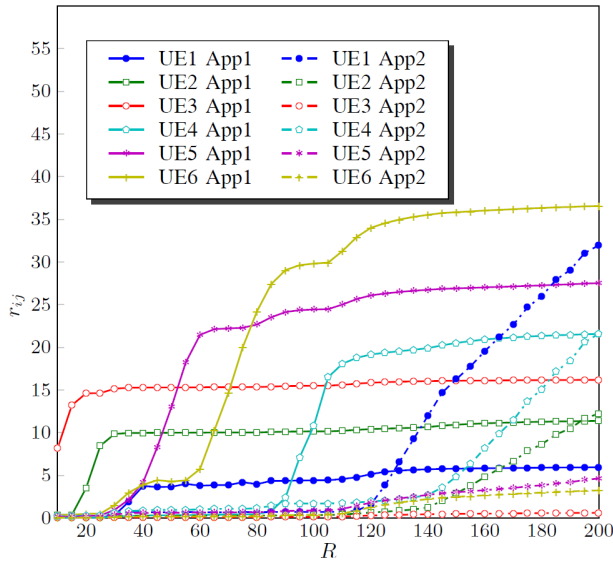


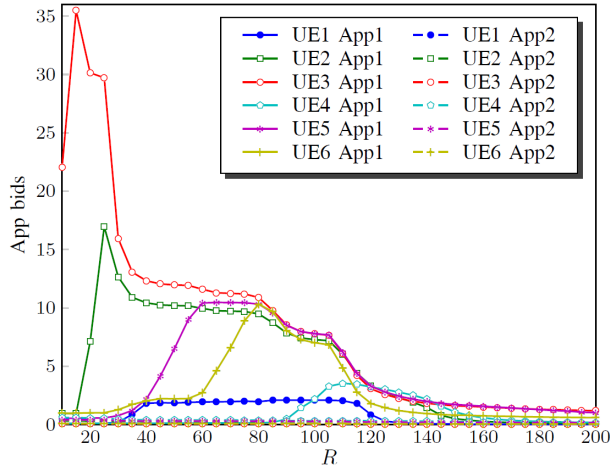
Fig. 5. Figure 5(a) depicts the optimal rates allocated to the UEs by the distributed scheme vs. eNB resources. No user is dropped as no assignment is zero. Figure 5(b) illustrates the UE bids for acquiring the resources vs. the eNB rate. The applications requiring more resources bid higher. When bandwidth is scarce, applications needing more resources bid significantly higher than the others. The plots reveal that the higher bid are tantamount to receiving more resources.

when the resources are scarce. In fact, we can see that the bid values for the delay-tolerant applications is significantly less than those of the real-time ones such that they are very close to the horizontal axis in Figure 6(b). Furthermore, those applications with higher QoS requirements such as the real-time streaming video in UE1 (red plot) bid higher in order to gain more bandwidth. However, as more resources become available at the eNB, bid values slash down as well.

On the contrary, the centralized resource allocation (Algorithms V.1 and V.2) assigns the application rates directly by the eNB, and the rates and bids are equal to the ones allocated by the distributed allocation in conformance to the theorem VI.3. Running the simulations, we got the same rate and bid diagrams as in the in Figures 6(a) and 6(b). It is notable that since utility proportional fairness objective functions are leveraged in the formation of the optimizations in equations (4), (5), and (6), both the distributed and the



(a) Application Optimal Rates



(b) Application Bids

Fig. 6. Figure 6(a) depicts the optimal application rates r_{ij} vs. the eNB rate R . Applications running on an UE are identically colored. As we can see, real-time applications are initially allocated more resources as opposed to the delay-tolerant ones due to their urgent need for resources. Figure 6(b) illustrates the applications bids in the UEs. The real-time applications bid higher when the resources are scarce, while the opulence of eNB resources escalates the application rates and reduces the UE bids.

centralized algorithms do not assign a zero rate to any UEs, thereby no user is dropped and a minimum QoS is warranted. As we mentioned before, an eNB allocates the majority of the resources to the real-time applications until they reach their utility inflection rate $r_{ij} = b_{ij}$. However, when the total eNB rate exceeds the inflection point rates sum $\sum b_{ij}$ of all real-time applications incumbent in the system, eNB can allot more resources to the delay-tolerant applications with ease of mind. This behavior is observed with the rate increase and bid value plummet that take place after the eNB rate surpasses the inflection points sum, i.e. $R = \sum b_{ij} = 105$, in Figure 6(a).

Furthermore, the improvement in the Algorithms IV.3 and IV.4 over the Algorithms IV.1 and IV.2 can be observed in the fluctuation reduction of the shadow price depicted in Figure 4(b), in which the decay function stabilizes the rate allocation

by eliminating oscillations. Such an allocation behavior is similarly seen for Algorithm IV.3 and IV.4 over Algorithm IV.1 and IV.2 for $R > \sum b_{ij} = 105$, but Algorithm IV.3 and IV.4 fails to assign the optimal rates and bids for $R < \sum b_{ij} = 105$. Therefore, Algorithm IV.3 and IV.4 is robust under scarce resource availability circumstances.

Next, section VII-B discusses the pricing capability of the proposed resource allocation modi operandi, and presents germane simulation results.

B. Pricing for $10 \leq R \leq 200$

As we explained before, Figure 6(a) shows the final rates and bids of different applications with varying eNB bandwidth, and the applications bids are proportional to the allocated rates. For example, the real-time applications (sigmoidal utilities) bid higher when the eNB resources are scarce and their bids reduce as R increases. Therefore, the pricing, proportional to the bids, is *traffic-dependent* which outfits service providers with the option to escalate the service price for their subscribers when the traffic load on the system is high. Thereby, service providers can motivate mobile subscribers to utilize the network when the traffic load is low in that they will be paying less for the same services by using the network during off-peak hours.

The shadow price $p(n)$, representing the total price per unit bandwidth for all users and applications, is illustrated in Figure 7 when eNB rate changes. As we can observe, the price is high under high-traffic situations, implied by a fixed number of users with less available resources (R is small), and it decreases for low-traffic circumstances when the same number of users have the luxury of more resources (R is large). It is particularly noticeable that large plummets in the shadow price occur after $R = \{15, 25, 85, 105\}$ which are essentially the points at which the rate for one of the real-time application utilities exceeds that of its inflection point. Furthermore, a large decrease is visible at the sum of the inflection points, i.e. $\sum_{i=1}^k r_{ij}^{\text{inf}}$. Here, $k = \{1, 2, \dots, M\}$ is the users index, M is the number of users, and i is the user with the maximum utility slope $\arg \max_i S_i(r_i)$, in our case user 3 ($b_{3j} = 15$) followed by user 2 ($b_{2j} = 10$) then the three users 1, 5, 6 which have almost the same $S_i(r_i)$ ($b_{1j} = 5, b_{5j} = 25, b_{6j} = 30$), and ultimately user 4 ($b_{4j} = 20$). The larger the difference between slopes $\Delta S_{ij} = |S_i(r_i) - S_j(r_j)|$, the higher the change in the shadow price $p(n)$ plot vs. R .

VIII. CONCLUSION

In this paper, we introduced a novel QoS-minded centralized and a distributed algorithm for the resource allocation within the cells of cellular communications systems. We formulated the centralized and distributed approaches as respectively a singular and double utility proportional fairness optimization problems, where the former allocated running applications rates directly by the allocation entity such as an eNB in response to the UE utility parameters sent, whereas the latter assigned the UE rates by the eNB in its first stage followed by the application rate allocation by the UEs in its second stage. Users ran both delay-tolerant and real-time applications

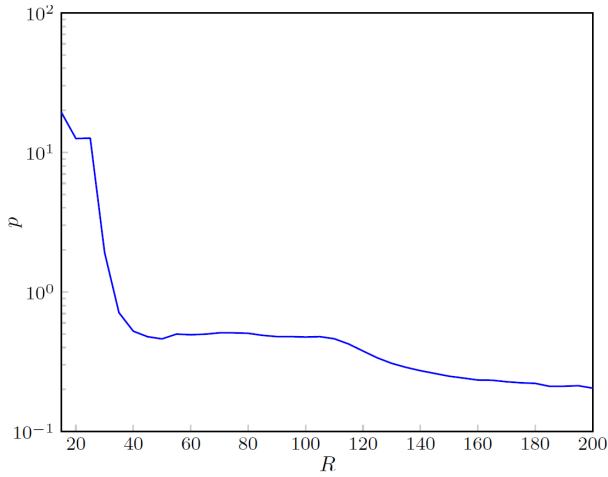


Fig. 7. Shadow Price p vs. eNB Resources R : Availability of more eNB resources reduces the shadow price.

mathematically modelled correspondingly as logarithmic and sigmoidal utility functions, where the function values represented the applications QoS percentage. Both of the proposed resource allocation formulations incorporated the service differentiation, application status differentiation modelling the applications usage percentage, and subscriber differentiations amongst subscribers priority within networks into their formulation. Not only did we prove that the proposed resource allocation problems were convex and solved them through Lagrangian of their dual problems, but also we proved the optimality of the rate assignments and the mathematical equivalence of the proposed distributed and centralized resource allocation schemes. Furthermore, we proved the mathematical equivalence of the distributed and centralized approaches by showing the both methods yield in identical optimal rates and pledged bids during their resource allocation processes.

Furthermore, we analyzed the algorithm convergence under varying sums of resources available to the eNB and introduced robustness into the distributed algorithm by incorporating decay functions into the aforementioned algorithm so that it converged to optimal rates for both high and low traffic loads occurring during the day by damping the rate assignment fluctuations resulting from scarcity of resources that appeared particularly in peak-traffic circumstances.

REFERENCES

- [1] M. Ghorbanzadeh, A. Abdelhadi, A. Amanna, J. Dwyer, and T. Clancy, "Implementing an optimal rate allocation tuned to the user quality of experience," in *IEEE International Conference on Computing, Networking and Communications (ICNC) Workshop CCS*, 2015.
- [2] "Ericsson mobility report," in *Ericsson Press Release*, 2013.
- [3] H. Ekstrom, "Qos control in the 3gpp evolved packet system," *IEEE Communications Magazine*, 2009.
- [4] M. Ghorbanzadeh, Y. Chen, K. Ma, C. Clancy, and R. McGwier, "A neural network approach to category validation of android applications," in *IEEE Conference on Computing, Networking, and Communications (ICNC)*, 2013.
- [5] S. Boyd and L. Vandenberghe, *Introduction to convex optimization with engineering applications*. Course Reader, 2001.
- [6] F. Kelly, A. Maulloo, and D. Tan, "Rate control in communication networks: shadow prices, proportional fairness and stability," in *Journal of the Operational Research Society*, 1998.

- [7] S. Low and D. Lapsley, "Optimization flow control, i: Basic algorithm and convergence," *IEEE/ACM Transactions on Networking*, 1999.
- [8] S. Shenker, "Fundamental design issues for the future internet," *IEEE Journal on Selected Areas in Communications*, 1995.
- [9] J. Lee, R. Mazumdar, and N. Shroff, "Non-convex optimization and rate control for multi-class services in the internet," *IEEE/ACM Transactions on Networking*, 2005.
- [10] J. Lee, R. Mazumdar, and N. Shroff, "Downlink power allocation for multi-class wireless systems," *IEEE/ACM Transactions in Networking*, 2005.
- [11] A. AbdelHadi and C. Clancy, "A Utility Proportional Fairness Approach for Resource Allocation in 4G-LTE," in *IEEE International Conference on Computing, Networking, and Communications (ICNC), CNC Workshop*, 2014.
- [12] A. Abdelhadi and C. Clancy, "A Robust Optimal Rate Allocation Algorithm and Pricing Policy for Hybrid Traffic in 4G-LTE," in *IEEE International Symposium on Personal, Indoor, and Mobile Radio Communications (PIMRC)*, 2013.
- [13] A. Abdelhadi, C. Clancy, and J. Mitola, "A resource allocation algorithm for users with multiple applications in 4g-lte," in *ACM Workshop on Cognitive Radio Architectures for Broadband (MobiCom Workshop CRAB)*, 2013.
- [14] R. Kurre, "Resource allocation for smart phones in 4g lte advanced carrier aggregation," Master Thesis, Virginia Tech, 2012.
- [15] H. Shajaiah, A. Abdelhadi, and C. Clancy, "Spectrum sharing between public safety and commercial users in 4g-lte," in *IEEE International Conference on Computing, Networking and Communications (ICNC)*, 2014.
- [16] H. Shajaiah, A. Abdelhadi, and T. Clancy, "Utility proportional fairness resource allocation with carrier aggregation in 4g-lte," in *IEEE Military Communications Conference (MILCOM)*, 2013.
- [17] H. Shajaiah, A. Abdelhadi, and C. Clancy, "Multi-application resource allocation with users discrimination in cellular networks," in *IEEE International Symposium on Personal, Indoor and Mobile Radio Communications (PIMRC)*, 2014.
- [18] H. Shajaiah, A. Abdelhadi, and C. Clancy, "Utility proportional fairness resource allocation with carrier aggregation in 4g-lte," in *IEEE International Conference on Computing, Networking and Communications (ICNC) Workshop CCS*, 2015.
- [19] G. Tychoiorgos, A. Gkelias, and K. Leung, "A new distributed optimization framework for hybrid adhoc networks," in *GLOBECOM Workshops*, 2011.
- [20] T. Harks, "Utility proportional fair bandwidth allocation: An optimization oriented approach," in *QoS-IP*, 2005.
- [21] G. Tychoiorgos, A. Gkelias, and K. Leung, "Utility proportional fairness in wireless networks," IEEE International Symposium on Personal, Indoor, and Mobile Radio Communications (PIMRC), 2012.
- [22] T. Nandagopal, T. Kim, X. Gao, and V. Bharghavan, "Achieving mac layer fairness in wireless packet networks," in *Proceedings of the 6th annual International Conference on Mobile Computing and Networking (Mobicom)*, 2000.
- [23] M. Ghorbanzadeh, A. AbdelHadi, and C. Clancy, "A utility proportional fairness approach for resource block allocation in cellular networks," in *IEEE International Conference on Computing, Networking and Communications (ICNC)*, 2015.
- [24] T. Erpek, A. Abdelhadi, and C. Clancy, "An optimal application-aware resource block scheduling in lte," in *IEEE International Conference on Computing, Networking and Communications (ICNC) Workshop CCS*, 2015.
- [25] M. Ghorbanzadeh, A. AbdelHadi, and C. Clancy, "A utility proportional fairness bandwidth allocation in radr-coexistent cellular networks," in *Military Communications Conference (MILCOM)*, 2014.
- [26] T. Jiang, L. Song, and Y. Zhang, "Orthogonal frequency division multiple access fundamentals and applications," in *Auerbach Publications*, 2010.
- [27] M. Ghorbanzadeh, Y. Chen, and C. Clancy, "Fine-grained end-to-end network model via vector quantization and hidden markov processes," in *IEEE Conference on Communications (ICC)*, 2013.
- [28] A. Abdelhadi and C. Clancy, "Context-aware resource allocation in cellular networks," in *arXiv*, 2014.
- [29] A. Abdelhadi, A. Khawar, and C. Clancy, "Optimal downlink power allocation in cellular networks," in *arXiv*, 2014.
- [30] S. Boyd and L. Vandenberghe, *Convex Optimization*. New York, NY, USA: Cambridge University Press, 2004.